International Journal of Science and Research Archive

eISSN: 2582-8185

Cross Ref DOI: 10.30574/ijsra

Journal homepage: https://ijsra.net/

(RESEARCH ARTICLE)

Check for updates

Early fault identification of rolling element using IESCFFOgram

Rabindra Kumar Sahoo *, M Sudhahar and P Vijay Kumar

Department of Mechanical Engineering, PRIST University, Vallam Thanjavur, India.

International Journal of Science and Research Archive, 2023, 08(01), 367–382

Publication history: Received on 28 November 2022; revised on 11 January 2023; accepted on 14 January 2023

Article DOI: https://doi.org/10.30574/ijsra.2023.8.1.0022

Abstract

Early fault identification of the rolling element bearings remains difficult because the repetitive transient signature generated via localized incipient damage is easily submerged by various interference components and strong noise. Spectral coherence (SCoh) is a break- through approach for revealing the second-order cyclostationary of bearing faults by displaying the energy flow of vibration signal jointly in a two-dimensional plane comprising the resonance frequency and bearing fault frequency. Considering the non-uniformity of fault in- formation distribution in the whole spectral frequency band, the enhanced envelope spectrum (EES) obtained by integrating over the full spectral frequency band is vulnerable to strong background noise. Thus, how to identify an informative spectral frequency band for constructing a diagnostic improved envelope spectrum (IES) is crucial to accurately identify bearing faults. To address this issue, a feature- adaptive method called IES via Candidate Fault Frequency Optimization-gram (IESCFFOgram) is proposed to determine the in- formative spectral frequency band from SCoh for bearing fault diagnosis. The innovation of this method is to fully excavate the fault information hidden in the SCoh and adaptively determine the informative spectral frequency band according to the identified candidate fault frequencies. The proposed method is tested and validated on simulated signals, vibration datasets obtained from artificial fault bearing experiments, and accelerated bearing degradation tests. In addition, comparisons with state-of-the art methods have been conducted to highlight the superiority of the proposed methodology.

Keywords: Spectral frequency; Fault Detection; Filtering Algorithm; Kurtosis; Cyclostationarity; Infogram

1. Introduction

Rolling element bearing is a precise mechanical component of the modern industrial system [1]. It is affected by axial load, radial load, impact load, and various external excitations under harsh operating conditions, through which structural fatigue cracks can be easily induced in internal components. If appropriate maintenance strategies are not implemented in time, it is easy to cause the breakdown of the mechanical system, which may result in considerable economic losses. There- fore, incipient fault detection of the rolling element bearings is vital for ensuring the safety and reliability of the mechanical systems [2, 3].

The typical methods for rolling element bearing fault detection can be roughly considered as a cascade of the filtering algorithm and envelope spectrum (ES) analysis. The filtering algorithm is utilized to enhance the repetitive transients induced by the localized defects observed in bearings or determine the frequency band containing diagnostic information, whereas ES is applied for identifying the fault types and severity.

Blind deconvolution [4] is a typical filtering algorithm used to recover fault- related periodic or quasi-periodic impulses from raw vibration signals, in which a finite-impulse response filter is used to eliminate the influence of the transmission paths of various external signals and extract fault-related repetitive transient sig- natures by maximizing a certain criterion of the filtered signal. By considering kurtosis, D-norm, multi-D-norm, correlated kurtosis, and cyclostationarity

* Corresponding author: Rabindra Kumar Sahoo

indicators as the criteria to be maximized, blind deconvolution algorithms, such as minimum entropy deconvolution (MED) [4, 5], maximum correlated kurtosis deconvolution (MCKD) [5], multipoint optimal minimum entropy deconvolution adjusted (MO- MEDA) [6], and cyclostationarity-based blind deconvolution (CYCBD) [7], have been developed, respectively, for enhancing the fault-related repetitive impulses. Based on statistical optimization algorithms, Cheng et al. [8, 9, 10] proposed a new strategy for solving the deconvolution inverse filter and applied it to the ex- traction of weak fault features of bearings. The pioneered filtering algorithm used to determine informative frequency band is spectral kurtosis (fast kurtogram, FK) proposed by Antoni [11, 12, 13], in which the bandpass filtering is used to divide the vibration signal into different frequency bands; subsequently, the frequency band with the largest kurtosis is automatically selected for further analysis. In- spired by the FK algorithm, various frequency band selection algorithms, such as Protrugram [14], Autogram [15], Sparsogram [16], and average Inforgram [17], have been proposed for identifying the resonance frequency band of rolling bearing fault. In Protrugram, kurtosis of the ES of the demodulated signal is considered as the criterion for determining the informative frequency band; this method is more robust to non-Gaussian noise in comparison with FK. Unlike FK and Protrugram, Sparsogram/Inforgram measures the information level for fault detection based on the ratio of the L2 and L1 norms (L2/L1 norm)/Negentropy (NE) of the squared envelope/squared ES (SES) of the narrowband filtered signal. All these

methods exhibit a similar working mechanism, that is, a bandpass filter bank (e.g., wavelet packet filter bank [14, 16] or 1/3-binary tree filter bank [13, 17]) is initially used to divide the vibration signal into different frequency bands, and the optimal frequency band carrying information about the rolling element bearing faults is subsequently selected according to a specified sparsity indicator. In addition, sim- ilar frequency band selection methods have been developed and applied to bearing fault identification recently, such methods can be observed in works of literature [18, 19, 20].

Another effective method used as an alternative to the ES-based methods for bearing fault identification is the spectral correlation (SC)/spectral coherence (SCoh)–the normalized version of SC [21]. SC/SCoh is an important vibration signal analysis method that reveals the second-order cyclostationary of bearing faults by mapping the vibration signal into a two-dimensional plane comprising spectral frequency and cyclic frequency. The physical meaning of spectral fre- quency is identical to that of the frequency obtained via Fourier transformation, and cyclic frequency contains repetitive transient impulses frequency and its multipliers that need to be identified in bearing fault diagnosis. However, SC/SCoh involves advanced stochastic process theory and requires considerable calculation time in some cases, substantially preventing the wide application of the SC/SCoh for quickly solving fault diagnosis problems. To address this issue, a fast and effective SC estimator with suitable convergence performance and low complexity, i.e., the fast SC algorithm, was proposed by Antoni [22]. The fast SC algorithm is based on short-time Fourier transformation and uses the fast Fourier transform to evaluate the scanning cyclic frequency spectrum. The squared ES (SES)/enhanced ES (EES) generated by integrating SCoh over the full spectral frequency band is a suitable tool for extracting the bearing fault information, but sensitive to strong interference noise. Therefore, the spectrum obtained by integrating the SCoh over a certain spectral frequency band with rich fault information, namely improved ES (IES), was suggested to enhance the fault-related cyclic components and perform fault detection. Wang et al. [23] proposed an L2/L1 norm-based guideline for determining the informative spectral frequency band with a fixed bandwidth. In this method, a spectral frequency band with a bandwidth covering three times the inner race fault frequency is used to scan the entire spectral frequency band of SCoh. Further, it selects the frequency band with the largest L2/L1 norm as the optimal spectral frequency band for producing diagnostic IES. Schmidt et al. [24] proposed a signal-to-noise ratio-based indicator to determine an informative spectral frequency band for generating a narrowband IES from SCoh. Mauricio et al. [25] proposed IES via feature optimization-gram (IESFOgram) for rolling element bearing diagnostics under non-stationary operating conditions. In this method, the spectral frequency band is initially divided into a 1/3-binary tree structure and the informative narrow band for generating IES is selected according to a fault characteristic frequency (FCF) based diagnostic feature. This method has been applied to the vibration signal analysis of rotating machinery and has achieved effective diagnostics performance under different conditions [26, 27, 28, 29]. Similarly, Chen et al. [30]developed an FCF-based method to identify the optimal spectral frequency band of the SCoh for bearing fault detection, and systemati- cally compared the performances of various blind and target features under the framework of IESFOgram. Furthermore, Zhang et al. [31] proposed an FCF-based strategy to construct the envelope spectrum tool by integrating the SCoh over the full spectral frequency band with weights. However, small fluctuations of the shaft speed around the nominal speed may hurt the FCF-based methods, and even result in poor fault detection capability. Therefore, a more robust method that does not rely on sparsity indicators and FCF is required for adaptively guiding the generation of an IES from the SCoh for bearing fault detection.

Hence, a feature-adaptive method called IES via Candidate Fault Frequencies Optimization-gram (IESCFFOgram) is proposed to identify the informative spectral frequency band from SCoh for bearings fault diagnosis in this project. In the new method, the candidate fault frequencies (CFFs) instead of the nominal FCF are automatically identified based on the local features of the SCoh and further used to guide the selection of the informational band. This new method

completely gets rid of the dependence on FCF or sparsity indicators and can adaptively gener- ate diagnostic IES by excavating the fault information hidden in the SCoh plane. Therefore, the proposed IESCFFOgram is suitable for the fault identification of rolling bearings under complex operating conditions. The simulated signals, vibration datasets obtained from artificial fault bearing experiments, and accelerated bearing degradation tests are served to illustrate the effectiveness and superior- ity of the proposed methodology for adaptively generating the IES and enhancing weak bearing fault diagnosis.

2. Problem Identification

Generally, the localized damage on rolling element bearings tends to arouse cyclic transient signatures under constant-speed conditions. Identification of the cyclic transient signatures from the measured vibration signal is the major part associated with the detection and tracking of localized defect evolution. SC is an effective approach for revealing the second-order cyclostationary of bearing faults by mapping the vibration signal into a two-dimensional plane comprising spectral and cyclic frequencies. Let $x(t_n)$ be a vibration signal of faulty bearings, where $t_n = n/F_s, n = 0,1, \dots, L-1$ is the discrete-time series and F_s is the sampling frequency. According to the cyclostationary theory, the instantaneous autocorrelation function of the bearing vibration signal comprises period T [22]:

$$R_x(t_n, \tau_m) = E\{x(t_n)x(t_n - \tau_m)^*\} = R_x(t_n + T, \tau_m) \dots\dots\dots\dots(1)$$

where E indicates the ensemble average operator, * indicates the complex conjugate, and $\tau_m = F_s$. SC is defined as the double discrete Fourier transform of the instantaneous autocorrelation function as follows [22]:

$$S_x(\alpha, f) = \underset{N\to\infty}{Lim} \frac{1}{(2N+1)F_s} \sum_{n=-N}^{N} \sum_{m=-\infty}^{\infty} R_x(t_n, \tau_m) e^{-j2\pi n\frac{\alpha}{F_s}} e^{-j2\pi m\frac{f}{F_s}} \dots\dots\dots(2)$$

The bivariate function $S_x(\alpha, f)$ quantifies the correlation level between two frequency components of the signal at f and $f + \alpha$, therefore can be interpreted as the decomposition of the analyzed signal concerning the “modulation frequency" α and “carrier frequency" f. It is continuous in the case of spectral frequency f and discrete in the case of cyclic frequency α when considering $x(t_n)$ to be a second-order cyclostationary signal [22]:

$$S_x(\alpha, f) = \begin{cases} S_x^k(f), & \alpha = k/T \\ 0, & \text{elsewhere} \end{cases} \dots\dots\dots\dots(3)$$

where, $S_x^k(f)$ $(k = 0, \pm1, \pm2, \dots)$ indicates the cyclic spectra. SCoh is the normalized version of the SC, wherein the amplitude is normalized between 0 and 1 [22]:

$$\gamma_x(\alpha, f) = \frac{S_x(alpha, f)}{\sqrt{(S_x(0,f)S_x(0,f-\alpha))}} \dots\dots\dots(4)$$

where, $S_x(0, f)$s the classic power spectral density. The SES is calculated by integrating the SCoh over the full spectral frequency band as follows:

$$SES(\alpha) = \frac{2}{F_s} \left| \int_0^{F_s/2} \gamma_x(\alpha, f) df \right| \dots\dots\dots(5)$$

In the case of the fast-rotating phases, integration of the complex values $\gamma_x(\alpha, f)$ may converge toward zero, resulting in the loss of bearing damage signature information [22]. To address this problem, adjusting the Equation 5 to integrate the modulus of SCoh along the spectral frequency axis delivers the so-called EES as follows [22]:

$$EES(\alpha) = \frac{2}{F_s} \left| \int_0^{F_s/2} \gamma_x(\alpha, f) df \right| \dots\dots\dots\dots(6)$$

The integration’s in Equations 5 and 6 are replaced by the discrete sum of the spectral frequency f for fast numerical calculation. In the case of weak bearing fault characteristics, the high-level noise, and strong interruptions from other cyclic frequencies in full-band EES are likely to dominate the entire EES and considerably submerge the bearing diagnostic information. Thus, a more sensible and effective approach is to implement spectrum analysis by integrating the modulus of SCoh over a specific spectral frequency band carrying diagnostic information for rolling element bearing fault detection.

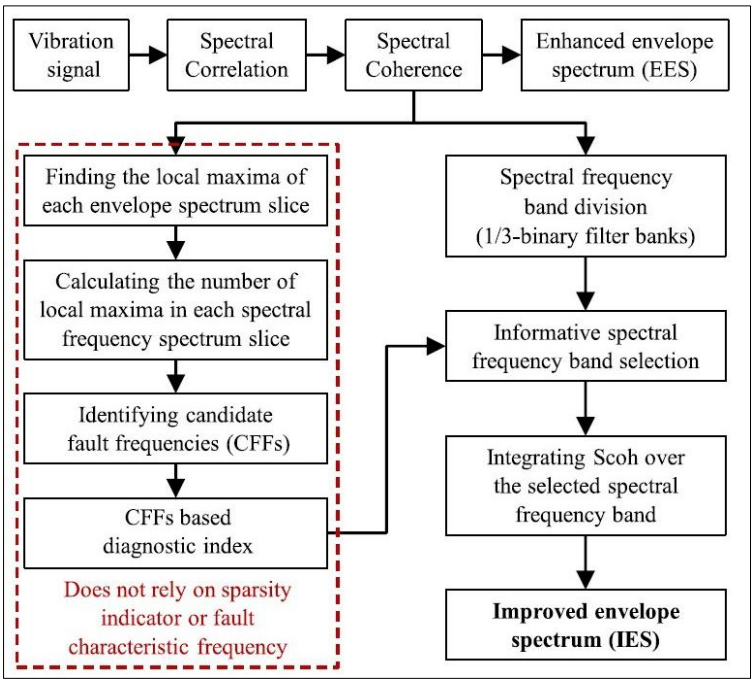

Figure 1 Schematic description of the EES, IES, and the proposed AWCES

3. Methodology & Flow chart

3.1. IESviaCandidateFaultFrequenciesOptimization- gram (IESCFFOgram)

In this subsection, a feature-adaptive method called IES via Candidate Fault Frequencies Optimization-gram (IESCFFOgram) is proposed to discriminate the in- formative band from SCoh for bearing fault diagnosis. First, the local extrema of the cyclic frequency spectrum slices (CFSSs) on SCoh is employed to identify the cyclic frequencies that may be induced by the local defects of rolling element bearings, which is called candidate fault frequencies (CFFs) in the project. Then, the ratio of the energy of all CFFs to the energy of IES is applied as an indicator to quantify the level of fault information of each narrowband divided from full spectral frequency band using 1/3-binary tree filter banks. Last, the narrowband IES with the largest RE is selected as the optimal spectrum tool to perform bearing fault diagnosis. Figure 1 presents the flowchart of the proposed IESCFFOgram for generating IES from SCoh for bearing fault detection.

3.1.1. Identification of CFFs

Repeating the original intention of SCoh, the amplitude of $\gamma_x(\alpha, f)$ has a clear physical significance–to quantify the correlation between two frequency components of the bearing vibration signal at f and f + α. The vibration signal $x(t_n)$ exhibits pure second-order cyclostationarity at α if its SCoh $\gamma_x(\alpha, f)$ has non-zero values along lines parallel to the spectral frequency axis in the (α, f) plane, that is, the spectral frequency spectrum slice (SFSS) $\gamma_x(\alpha, .)$ has nonzero values. Due to the presence of interference signal components (such as discrete harmonics, background noise, etc.), the measured vibration signal often exhibits mixed cyclostationarity rather than the pure second-order cyclostationarity. The direct result of this fact is that even if the vibration signal has no pure tone at cyclic frequency α, the SFSS at cyclic frequency α $\gamma_x(\alpha, .)$ may have a non-zero value along the spectral frequency axis. The vibration signal exhibiting second-order cyclostationary at frequency α is often manifested as a series of local maxima distributed on some CFSSs parallel to the cyclic frequency axis. Extensive usage of the information regarding local maxima on all CFSSs can help to develop a narrowband IES indicating the presence of modulations and facilitating the identification of fault frequencies.

Assume that $\gamma_x^{est}(\alpha, f)$ is the estimator of $\gamma_x(\alpha, f)$ with an equidistant discrete spectral frequency $f_g = g.F_s/N_w, g = 0, \dots, N_w - 1$ and equidistant discrete cyclic frequency $\alpha_1, \alpha_2, \dots, \alpha_N = \alpha_{max}$ For any spectral frequency f_g, defining $\xi_x(n, g), n = 1, \dots, N$ as a binary variable determined by the local maxima distribution of the g^{th} CFSS $\xi_x^{est}(., f_g)$ such that:

$$\xi_x(n,g)=\begin{cases}1 & if L\le n\le N-L and \xi_x^{est}(\alpha_{n+l},f_g), l=\pm1,\dots,\pm L\\ 0 & elsewhere\end{cases}\text{.....(7)}$$

where L (recommended to have a value of 3–5) is a parameter controlling the sparsity of the local maxima on CFSSs. The nonzero elements in the matrix $\xi=(\xi_x(n,g))_{N\times N_w}$ correspond to the local maxima of CFSSs on the entire SCoh plane. If α_n is a fault-related frequency (e.g. FCF or its multiples, sidebands) attributed to the localized defect on the rolling element bearings, the majority of the CFSSs have relatively larger amplitudes at this cyclic frequency α_n than those determined in its neighborhood, indicating that the matrix xi contains more nonzero elements in the nth row. Therefore, the rows of the matrix ξ with more nonzero elements correspond to the cyclic frequencies more likely to be caused by the localized defects on rolling element bearings. To capture this key information, let $\eta=[\eta(1),\eta(2),\dots,\eta(N)]^T$ be a vector delivered by summing the row vectors of the matrix ξ as follows:

$$\eta(n)=\sum_{m=1}^{M}\xi(n,m), n=1,2,\dots,N\text{.....(8)}$$

The n^{th} element $\eta(n)$ quantifies the number of local maxima contained in the n^{th} SFSS $\gamma_x^{est}(\alpha_(n),.)$. Let $\tilde{\eta}=[\widetilde{\eta_1},\widetilde{\eta_1},\dots,\widetilde{\eta_N}]^T$ be the arranged version of η satisfying the following conditions:

- For any i ≤ j, $\tilde{\eta_i}\ge\tilde{\eta_j}$ should hold.
- If $\tilde{\eta_i}=\widetilde{\eta_{i+1}}$ then, k_i and k_{i+1} should exist such that $\tilde{\eta}_i=\eta(k_i)$ and $\tilde{\eta}_{i+1}=eta(k_{i+1})$ and satisfying $SFSSAmp(k_i)>SFSSAmp(k_{i+1})$, where, $SFSSAmp(n)=\sum_{m=1}^{M}\xi_x(n,m).\gamma_x^{est}(\alpha_n,f_m)$

The function $SFSSAmp(n)$ quantifies the sum of the amplitudes of the local maxima contained in the n^{th} $SFSS\gamma_x^{est}(\alpha_n,.)$, and is used to solve the sorting problem of two or more equal elements in the vector η. The cyclic frequencies corresponding to the first D SFSSs with the most local maxima can be expressed as follows:

$$\widehat{\alpha(d)}=\{\alpha_n|\eta(n)=\tilde{\eta}_d, n=1,2,\dots,N\}, d=1,2,\dots,D\text{.....(9)}$$

The cyclic frequencies $\widehat{\alpha(d)}, d=1,2,\dots,D$ are defined as CFFs, which may be simultaneously composed of the fault-related and the interference frequencies. These CFFs are distributed on each CFSS and serve as the cornerstone for identifying IBF in the IESCFFOgram.

3.2. Proposed IESCFFOgram method

The proposed IESCFFOgram method combines the full spectral frequency band division strategy of the 1/3-binary tree filter structure and the diagnostic feature calculated from the identified CFFs to optimally discriminate the informative band of the specified fault type. For the i^{th} $(i=0,1,1.6,2,2.6,3,\dots)$ narrowband at the l^{th} level, the resulting IES is formulated as follows:

$$IES_{l,i}(\alpha)=\frac{1}{F_s/2^{l+1}}\int_{F_s(i-1)/2^{l+1})}^{F_s i/2^{l+1})}|\gamma_x(\alpha,f)df|\text{.....(10)}$$

Then, the ratio of the energy of all CFFs to the energy of $IES_{l,i}(\alpha)$, abbreviated as RE, as the diagnostic index to quantify the level of fault information hidden in $IES_{l,i}(\alpha)$. The diagnostic index $ER_{l,i}$ of $IES_{l,i}(\alpha)$is defined as follows:

$$ER_{l,i}=\frac{\sum_{n=1}^{N}I_{\hat{a}(d),d=1,2,\dots,D}(\alpha).|IES_{l,i}(\alpha_n)|^2}{\sum_{n=1}^{N}|IES_{l,i}(\alpha_n)|^2}\text{.....(11)}$$

where $I_{\{.\}(\alpha_n)}$ is the indicative function, which refers to a binary function with a value of 0 or 1 such that:

$$I_{\hat{a}(d),d=1,2,\dots,D}(\alpha_n)=\begin{cases}1 & if\alpha_n\in\{\hat{a}(d),d=1,2,\dots,D\}\\ 0 & if\alpha_n\notin\{\hat{a}(d),d=1,2,\dots,D\}\end{cases}\text{.....(12)}$$

A larger$ER_{l,i}$ indicates more information about CFFs hidden in $IES_{l,i}(\alpha)$. Finally, the IES with maximum diagnostic index is employed to perform bearing diagnostics. The IESCFFOgram and the corresponding scheme, consisting of the identification of CFFs and the selection of optimal diagnostic spectral frequency band, are presented in Fig 1. The detailed implementation procedure of the IESCFFOgram is described as follows:

- Estimate the SCoh of the bearing vibration signal following the fast SC algorithm [?] by setting the appropriate window length N_w and maximum cyclic frequency to scrutinize.
- Divide the full spectral frequency band of the SCoh into a set of narrow bands using the 1/3-binary tree structure strategy. Then, construct $IES_{l,i}(\alpha)$ by integrating the SCoh over the ith (i = 0, 1, 1.6, 2, 2.6, 3, …) narrow spectral frequency band at the l^{th} level.
- Identify the CFFs based on the distributions of local maxima of all CFSSs on the entire bivariate SCoh plane and further calculate the diagnostic index ER of the narrowband $IES_{l,i}(\alpha)$ by using Eq. 11.
- Select the IES with the maximum ER value as the optimal envelope tool to perform bearing fault diagnosis

4. Results and discussion

In this section, the diagnostic performance of IESCFFOgram is demonstrated on three bearing experimental datasets collected from different test rigs. Comparisons with ES, EES, average Infogram, and IESFOgram were conducted to highlight the superiority of the proposed method in adaptively identifying the informative spectral frequency band of SCoh.

4.1. Experimental verification 1: Bearing rolling element fault detection

In this section, the effectiveness of the proposed method is validated using experimental signals obtained from the Bearing Data Center of the Case Western Reserve University (CWRU) [32]. Fig.2 displays the experimental test rig used in this study comprising a 2HP and three-phase induction motor (left), torque sensor (middle), and dynamometer (right) connected through self-aligned coupling (middle). An accelerometer is mounted on the motor housing at the drive end of the motor for collecting the vibration signals produced by experimental bearings. The data collection system comprises a high-bandwidth amplifier, which has been particularly designed for vibration signals and a data recorder with a sampling frequency of 12 kHz per channel. Herein, the signal length is set to 11.0973 s for experimental analysis.

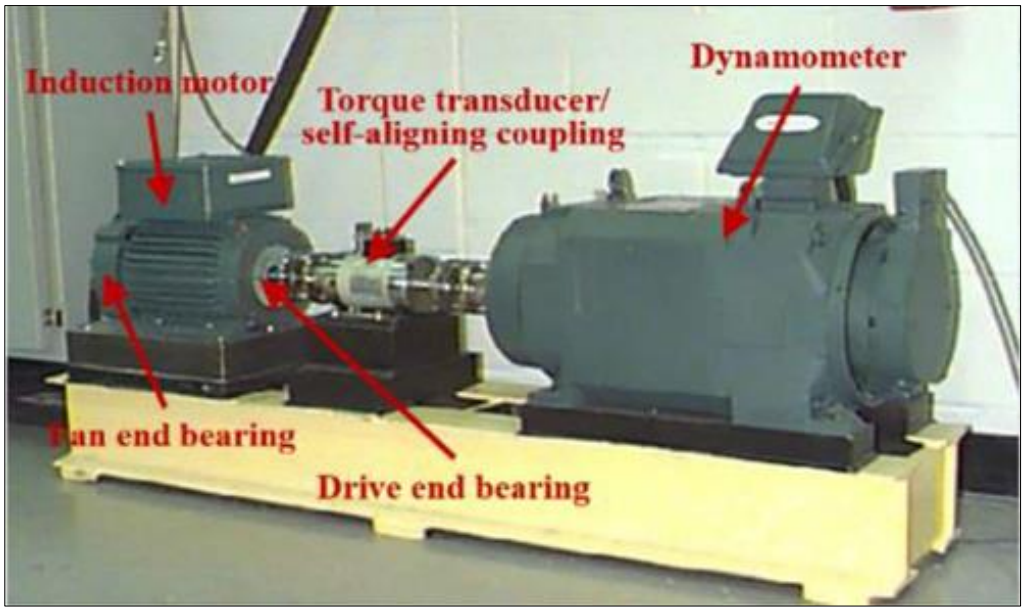

Figure 2 Case Western Reserve University Test Rig

The vibration signal of the fan-end bearing with a rolling element defect of 0.07 in collected at a shaft rotation speed of 1797 rpm is analyzed. The ball spin frequency (BSF) and cage characteristic frequency are 119.4 Hz and 11.4 Hz, respectively. Fig. 3 depicts the time-domain waveform and corresponding ES of the rolling element fault signal to be analyzed. As shown in Fig. 3(b), the ES of the raw vibration signal is composed of complex frequency components, and the BSF and its harmonics can hardly be discovered under the interferences of the surrounding spectral lines. Using SCoh to loosen the fault-related cyclostationary characteristics hidden in the vibration signal, the result is shown in Fig. 4(a), wherein the energy in the narrowband centered around 1700 Hz is relatively large. The EES of the SCoh plotted in Fig. 4(b) demonstrates that the raw vibration signal is contaminated by background noise below 400 Hz, causing the BSF and its harmonics to be invisible. Setting the parameter p1 to 2.5%, Fig. 4(c) displays the IESCFFOgram of the raw vibration signal, from which the identified informative spectral band is centered at 4125 Hz with a bandwidth of 250

Hz. Fig 4(d) depicts the IES of IESCFFOgram, wherein BSF and its first two harmonics are outstanding without intolerable interference spectrum lines around. The results obtained by using the average Inforgram (setting the decomposition level to four) to process the signal displayed in Fig. 3(a) are presented in Figs. 5(a) and (b). As observed in Fig. 5(b), amplitudes of BSF and its harmonics are completely concealed in the spectral lines. The results of the IESFOgram assisted with accurate FCF 119.4 Hz are presented in Fig. 5(c) and (d). Compared with IESCFFOgram, the frequency band selected by IESFOgram is narrower, and the informative frequency bands selected by these two methods coincide in [4000 Hz, 4125 Hz]. The IES depicted in Fig. 5(d) prominently shows the existences of BSF and its harmonics, which.

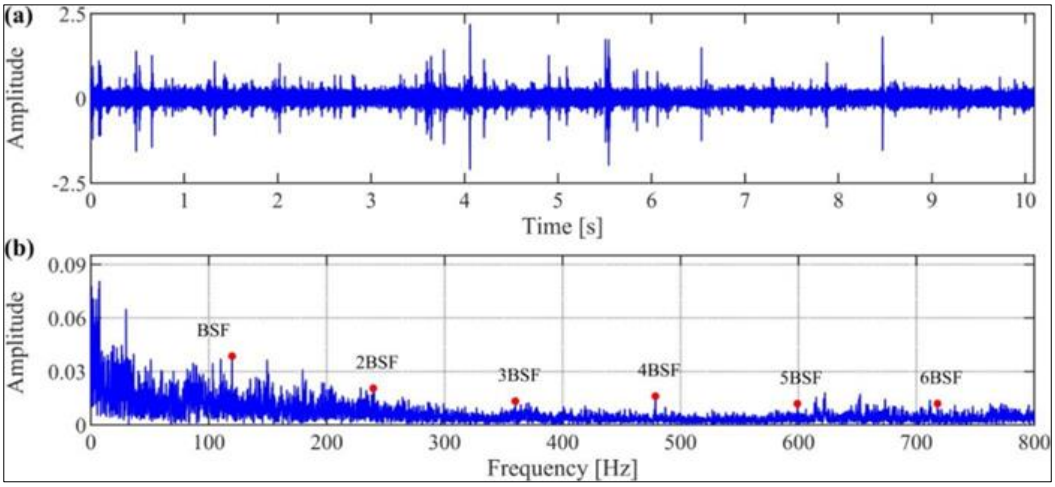

Figure 3 Raw rolling element fault signal and its envelope spectrum: (a) raw signal and (b) envelope spectrum

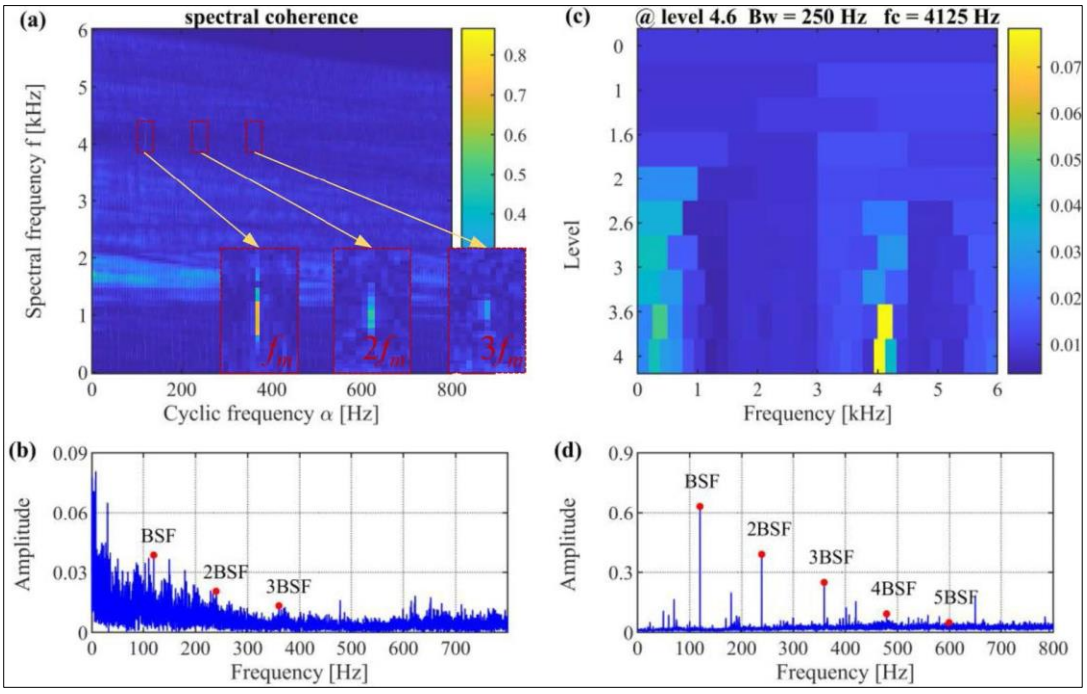

Figure 4 Results obtained from EES and IESCFFOgram (p1 = 2.5%): (a) SCoh; (b) EES from Scoh; (c) IESCFFOgram; (d) IES from IESCFFOgram

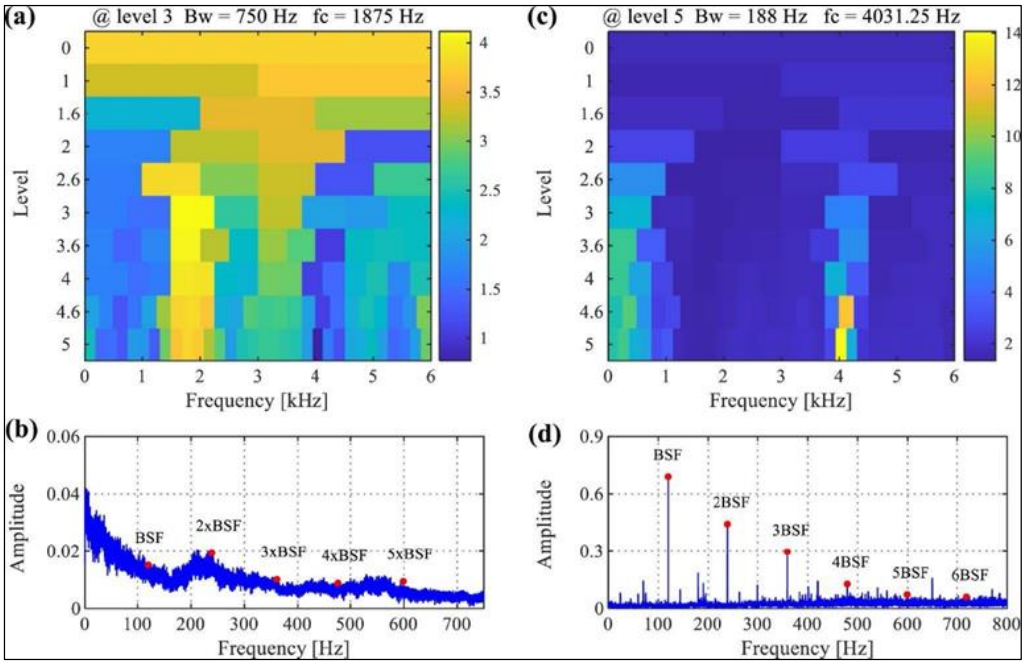

Figure 5 Results obtained from average Infogram and IESFOgram: (a) average Infogram and (b) its SES; (c) IESFOgram and (d) its IES

is similar to IES from the IESCFFOgram shown in Fig. 4(d). This subsection finally explores the robustness of IESCFFOgram and IESFOgram. Varying the parameter p1 from 1% to 10% with a step of 0.09/25, the ADF obtained by using IESCFFOgram to process the fan-end bearing signal plotted in Fig. 3(a) is presented in Fig. 6(a), in which the ADF only fluctuates slightly, reflecting the robustness of the IESCFFOgram to the parameter p1. Further, the robustness of the IESFOgram to the deviation of the FCF is conducted. Introducing a deviation in the FCF as follows:

$$\tilde{fm} = fm + \delta \ldots\ldots\ldots\ldots\ldots\ldots (13)$$

where parameter δ quantifies the deviation of FCF. Fig. 6(b) displays the ADFs of the IESFOgram for processing the fan-end bearing signal under different deviations. It shows that IESFOgram is sensitive to the deviation of the FCF to be interested, causing its ADF to drop sharply below 10 or even close to 5 when the parameter δ is far away from zero

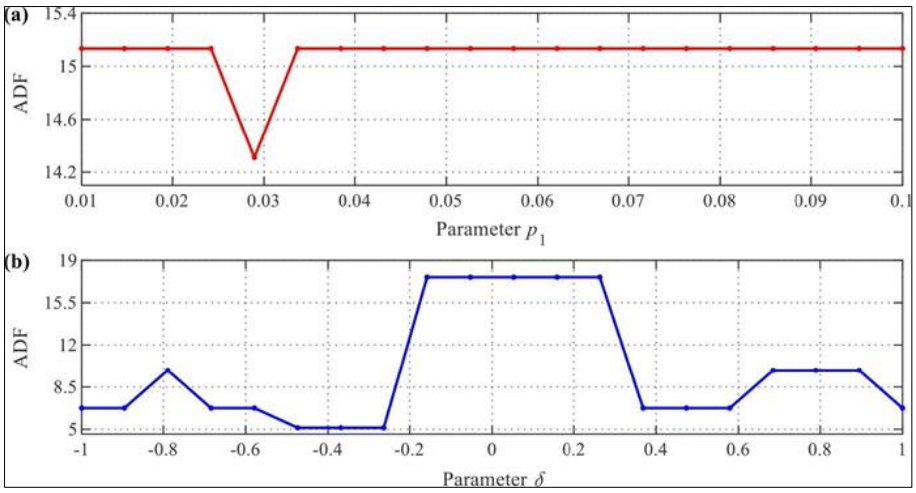

Figure 6 (a) ADFs of the IESCFFOgram for processing rolling element fault signal under different parameter p1; (b) ADFs of the IESFOgram for processing rolling element fault signal under different δ. Parameter H in ADF is specified as 6

4.2. Experimental verification 2: Bearing inner race fault detection

The second experimental dataset was collected from the bearing test rig of the University of Electronic Science and Technology of China (UESTC) [33]. The test rig is mainly composed of the motor and speed controller, support bearing, loading disk, and test bearing, as displayed in Fig. 7. A local defect was implanted into the inner race of the test bearing. During the experiment, the spindle was rotated at a constant speed of 3600 rpm (60 Hz), and the acceleration sensors were mounted on the housing of the faulty bearing to record the vibration data using a sampling frequency of 51.2 kHz. In this case, the ball passing frequency on the inner race (BPFI) of the faulty bearing is 325.8 Hz.

The time-domain waveform of the inner race fault signal and its ES are dis- played in Fig. 8, where the diagnostic information on the ES is not evident because of a large amount of interference spectral lines attributed to strong noise. Adjust- ing the maximum cyclic frequency αmax to 1200 to cover 3×PBFI, the SCoh for processing the raw inner race fault signal is plotted in Fig. 9(a), from which the resonance frequency band caused by bearing inner race fault cannot be directly observed. The EES from the SCoh is presented in Fig. 9 (b), wherein BPFI and its two harmonics can be identified; however, their corresponding amplitudes are relatively small. Setting the parameter p1 to 2.5%, results of the proposed IESCFFOgram method for dealing with the raw vibration signal are depicted in Fig. 9(c) and (d). The informative spectral band selected by IESCFFOgram is [6400 Hz.

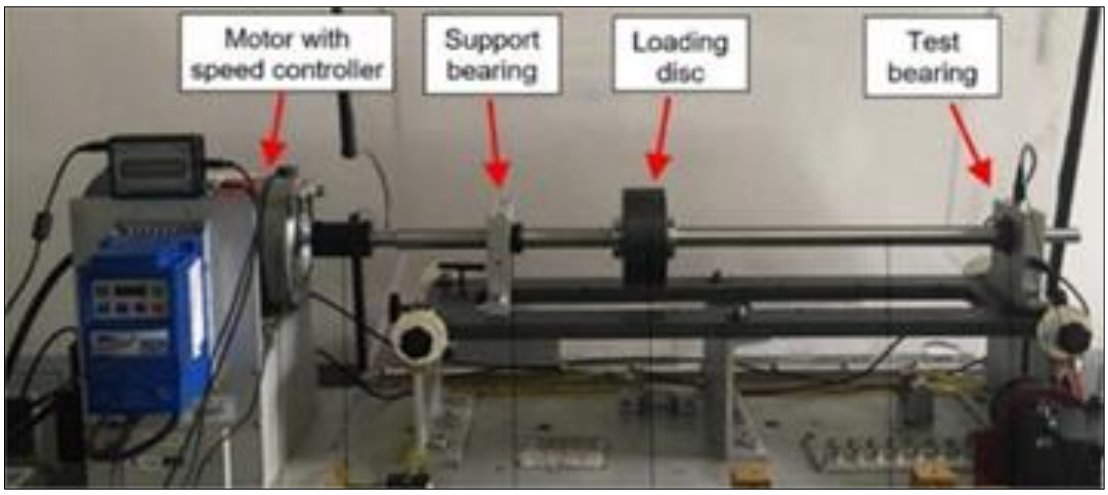

Figure 7 UESTC bearing test rig

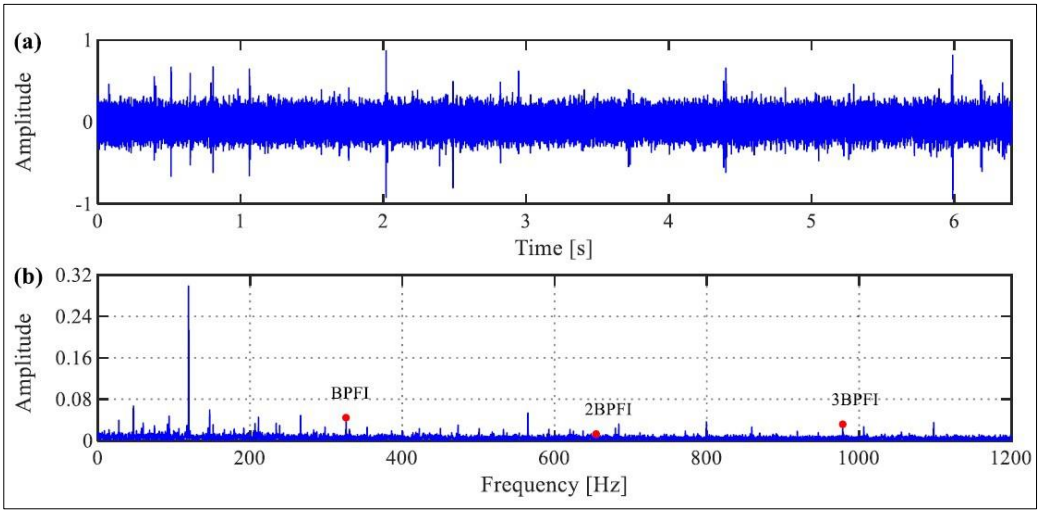

Figure 8 Raw inner race fault signal and its envelope spectrum: (a) raw signal and (b) envelope spectrum

7200 Hz], and the responding IES plotted in Fig. 9(d) provides more sufficient information about the defect on the bearing inner race when compared with that provided by the EES from SCoh.

The results of the average Inforgram obtained by specifying the decomposition level as five are displayed in Fig. 10(a) and (b). The SES determined by the average Inforgram is dominated by interference spectrum lines and does not carry diagnostic information. Taking the accurate BPFI as input, the IESFOgram and its IES are presented in Fig. 10(c) and (d), respectively. Similar to IESCFFOgram, the spectral frequency band [6400 Hz, 7200 Hz] is selected as an informative band by IESFOgram, indicating the same performances of these two methods in this case study.

Fig. 19(a) plots the ADFs obtained by IESCFFOgram for analyzing the inner race fault signal under parameter p1 changing from 1to 10%. This result demonstrates the surprising robustness of the proposed method to the key parameter p1. ADFs obtained by IESFOgram using the BPFI with deviation δ to analyze the inner race fault signal are depicted in Fig. 11(b), which shows that only the absolute deviation less than 0.2 Hz can guarantee the diagnostic performance of the IESFOgram.

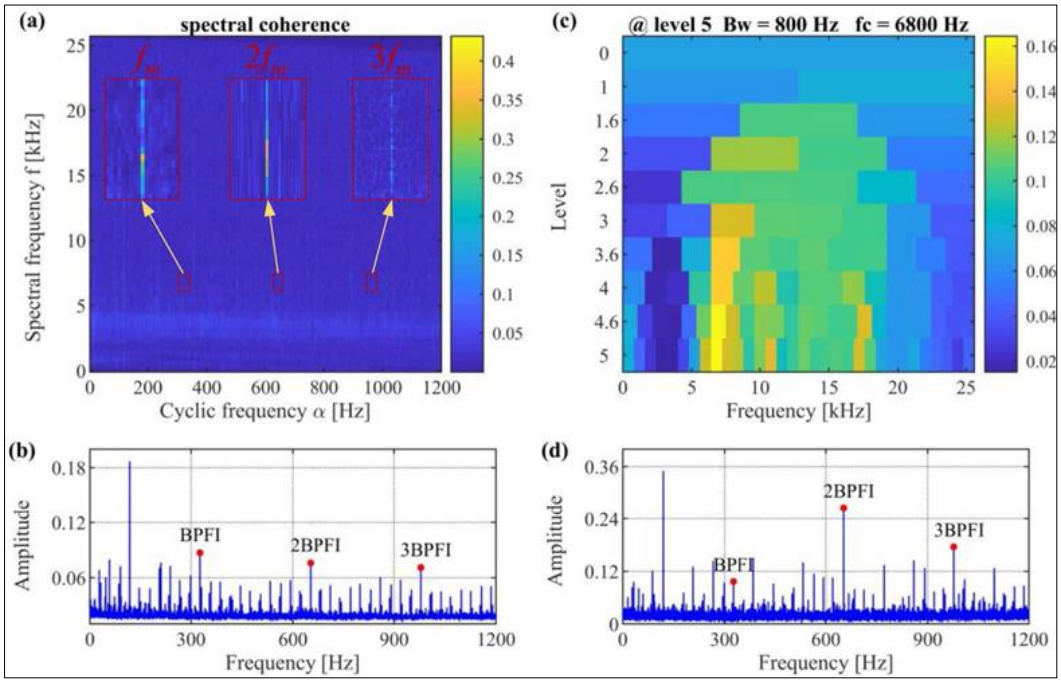

Figure 9 Results obtained from EES and IESCFFOgram (p1 = 2.5%): (a) SCoh; (b) EES from Scoh; (c) IESCFFOgram; (d) IES from IESCFFOgram

4.3. Experimental verification 3: Bearing outer race fault detection

At last, the bearing accelerated degradation datasets obtained from Xi'an Jiaotong University (XJTU), Shaanxi, China, and the Changxing Sumyoung Technology Co. Ltd. (SY), Zhejiang, China [34] are applied to demonstrate the performance of the proposed methodology in extracting incipient fault features. The tested bearings were of the LDK UER204 type and two PCB 352C33 accelerometers were mounted on the housing of the tested bearings to collect vibration data, as shown in the bearing test rig presented in Fig. 12. 15 rolling element bearings were tested under three different load conditions (10 kN, 11 kN, and 12 kN, respectively) until they completely failed. The sampling frequency was 25.6 kHz, and 32,768 samples (i.e., a single data segment of 1.28s) were recorded per minute.

The vibration signals of Bearing1-2, i.e. Bearing 2 under load 10kN, are an- alyzed in this subsection. A total of 161 sets of vibration signals were collected during the fatigue test lasting to 161min, at a rotation frequency of 35Hz and a localized defect was found on the outer race of the bearing at the end of the test. The ball passing frequency on the outer race (BPFO) is 107.8 Hz. Fig. 13

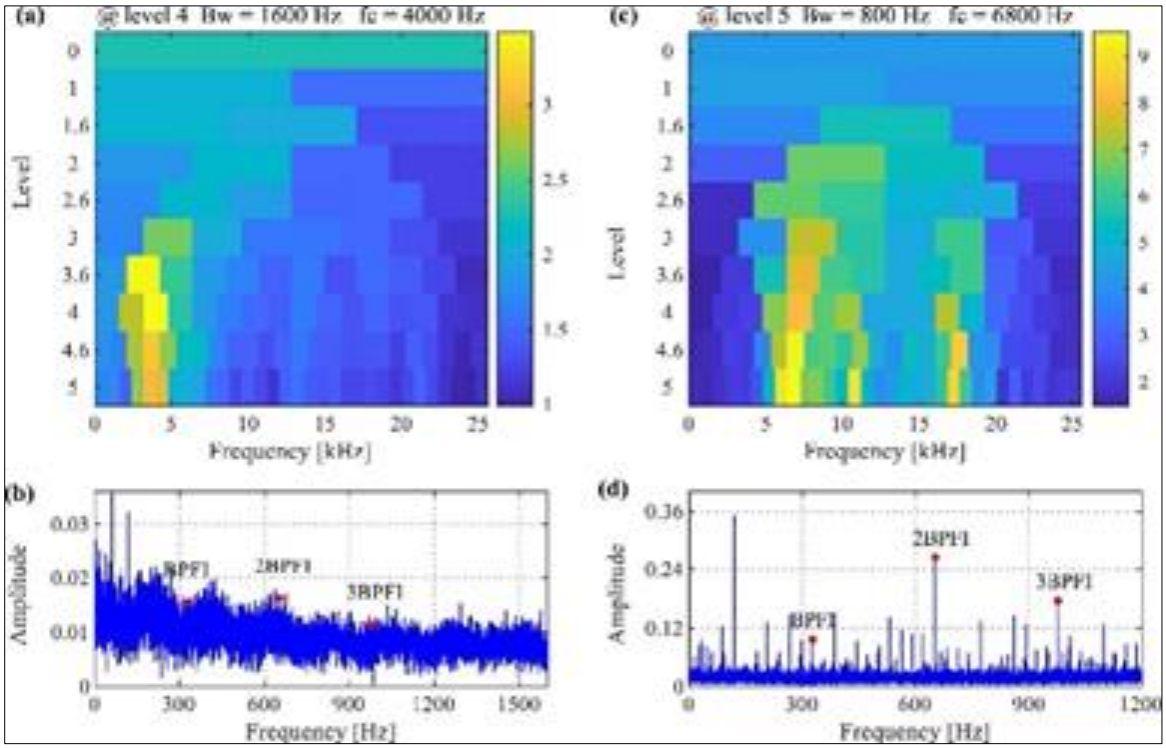

Figure 10 Results obtained from average Infogram and IESFOgram: (a) average Infogram and (b) its SES; (c) IESFOgram and (d) its IES

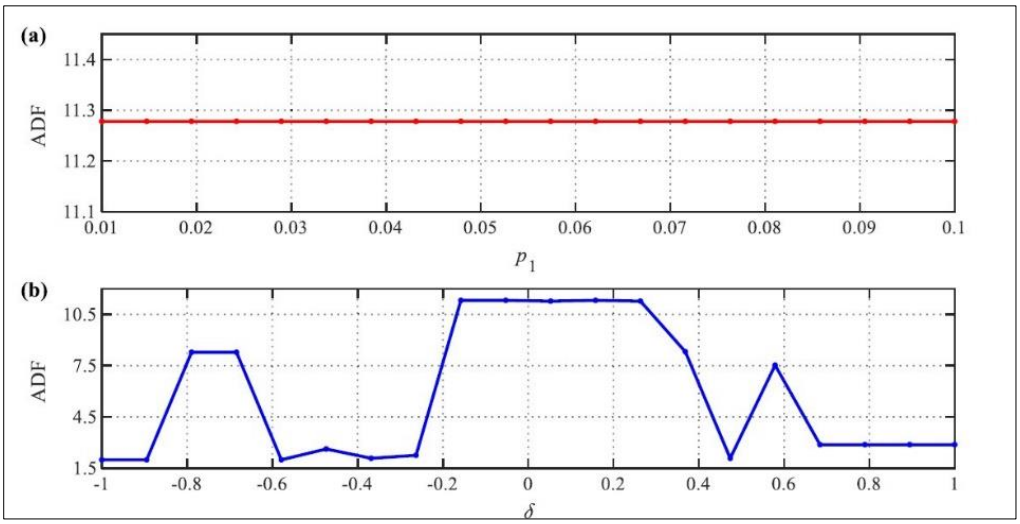

Figure 11 (a) ADFs of IESCFFOgram for processing inner race fault signal under different parameter p1; (b) ADFs of IESFOgram for processing rolling element fault signal under different parameter δ. Parameter H in ADF is specified as 3

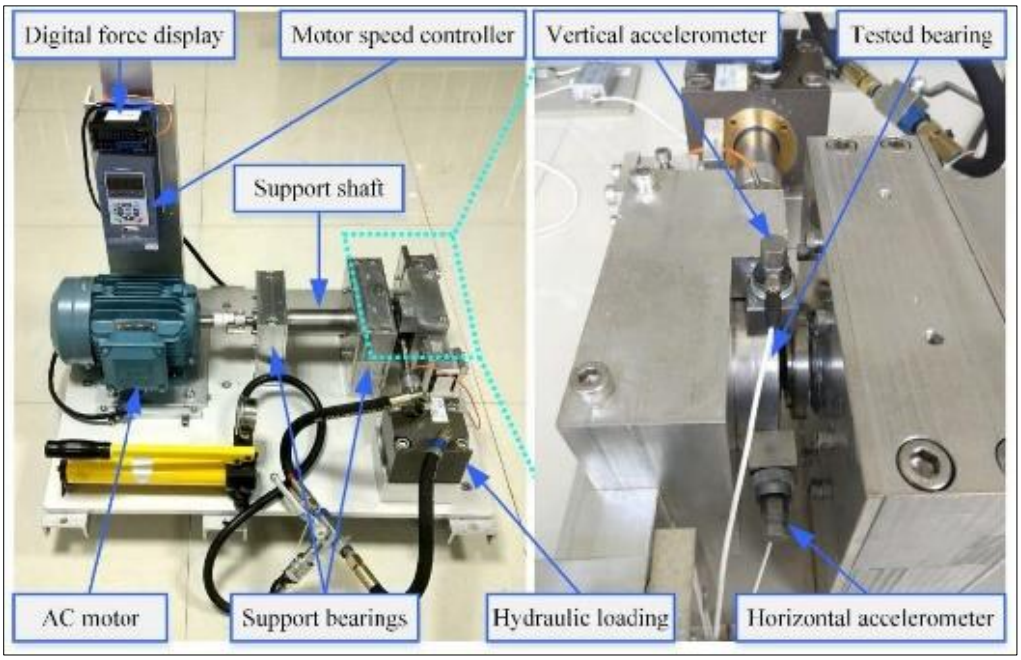

Figure 12 Bearing accelerated degradation test rig

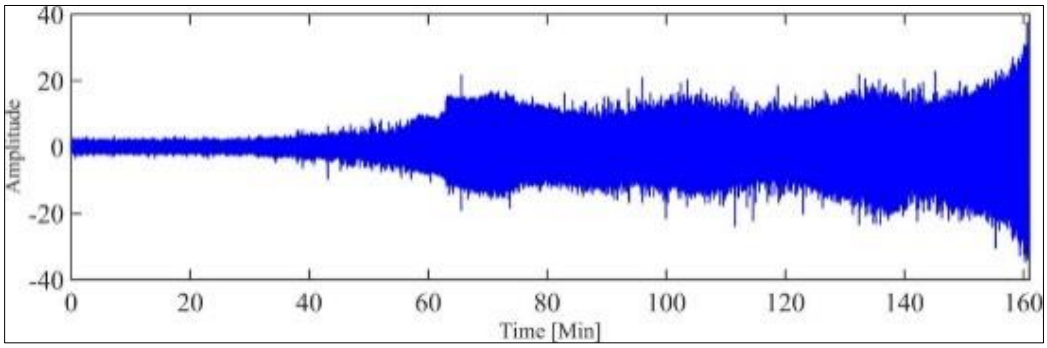

Figure 13 Accelerated degradation signals of Bearing1-2

Displays the accelerated degradation signals of Bearing1-2, in which the energy of the bearing vibration signal increased significantly one hour after the start of the test, indicating the deterioration of the bearing performance. Appling ES, EES, average Infogram, IESFOgram, and IESCFFOgram to detect the fault in- formation hidden in the raw vibration signals of Bearing1-2, the corresponding ADFs are presented in Fig. 14. Except for the average Infogram, the other four methods all detected the mutation of bearing performance at the 36th sampling point with a sharp increase in ADF. Compared with ES and EES, IESFOgram and IESCFFOgram exhibit better fault detection performance, judging from the ADFs determined by these two methods. In addition, without using FCF 107.8 Hz as input, the proposed IESCFFOgram has delivered the same ADF values as IESFOgram when analyzing the accelerated life datasets of bearing 1-2. To further compare IESFOgram and IESCFFOgram, the IESs of these two methods obtained by analyzing signals from the 28th to 40th samples are displayed in Fig. 15. The periodic flow of signal energy caused by the outer race fault is enhanced after the 32th sample signal, which is simultaneously detected by IESFOgram and IESCFFOgram in the form of the amplitudes of BPFO and its harmonics prominently appearing in IESs.

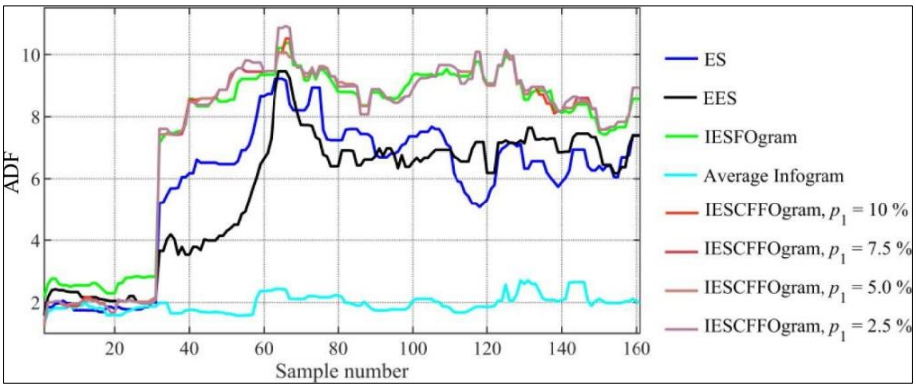

Figure 14 ADFs obtained by using different methods for processing the ac- celerated degradation signals of Bearing1-2. Parameter H in ADF is specified as 7

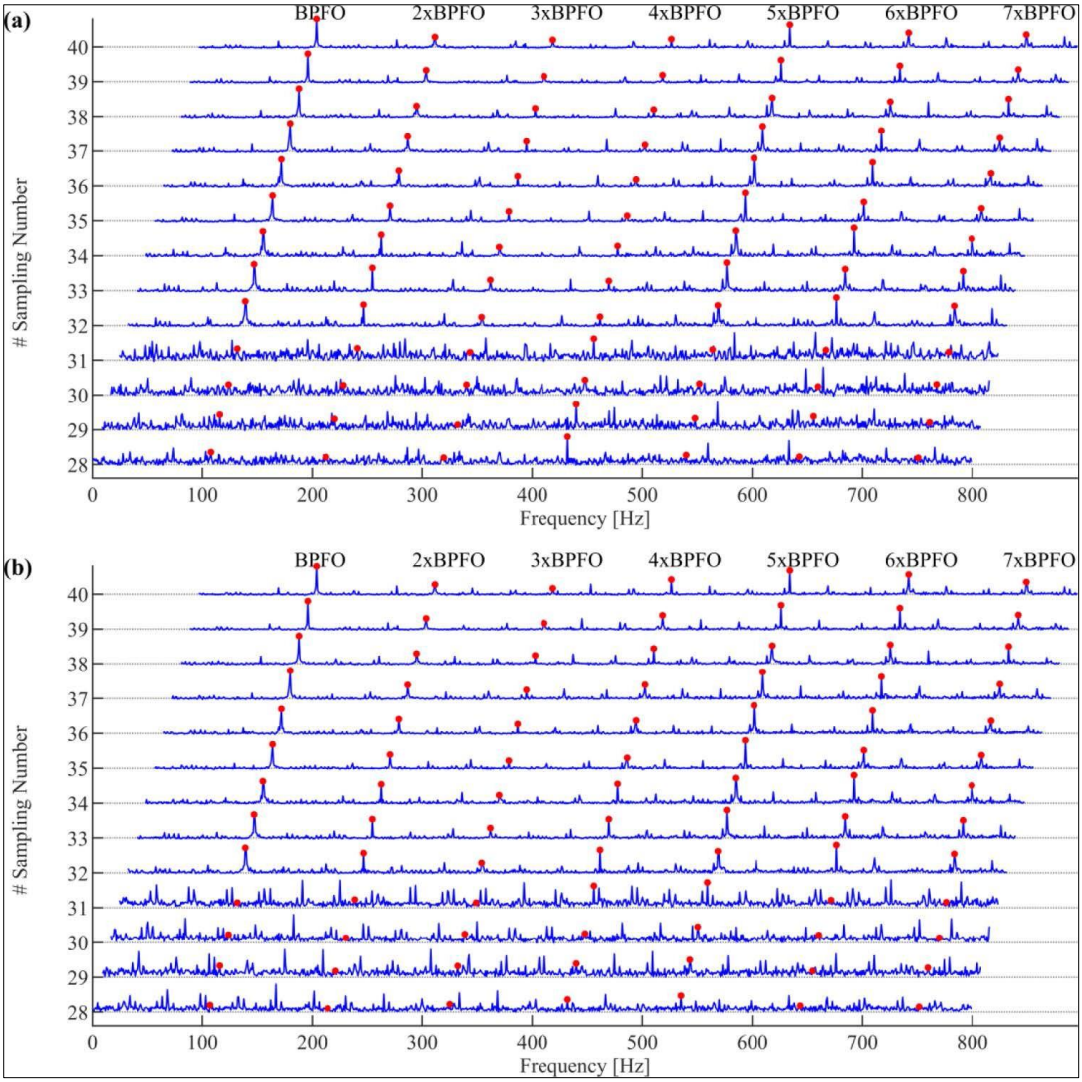

Figure 15 The IESs of the 32th to 40th sample signals of bearing1-2 obtained from: (a) IESFOgram (Setting p1 to 10%), and (b) IESCFFOgram (Using accurate BPFO as input)

5. Conclusion and Future scope

This paper proposes a feature-adaptive method called IESCFFOgram for generat- ing a narrowband IES from the SCoh for bearing fault diagnosis. The core and key innovation of this method is to use CFFs instead of nominal fault-related frequencies to identify informative frequency bands. First, a method using the local maximum information of the SCoh plane is designed to automatically identify CFFs without any prior information about bearing faults. Then, the 1/3-binary tree filter banks adopted by IESFOgram are applied to divide the spectral frequency band into a series of narrowband for generating candidate IESs, and a CFFs-dependent indicator called RE is utilized to quantify the fault information of the candidate IES. Last, the IES with the largest RE is served as the optimal spectrum tool for bearing fault diagnosis. The performance of the proposed IESCFFOgram is evaluated and verified using simulated signals, bearing experimental datasets, and bearing degradation dataset, accompanied by comparison analysis with EES from SCoh, SES from average Inforgram, and IES from IESFOgram. The following conclusions can be drawn from this study:

- The IESCFFOgram method can adaptively generate diagnostic IES on the basis of excavating the fault information hidden in the SCoh. Therefore, it is suitable for the fault identification of rolling bearings under complex operating conditions.
- The qualitative and quantitative analysis conducted on the simulated and experimental bearing datasets fully demonstrated the effectiveness and superiority of IESCFFOgram in comparison with EES and average Inforgram. Without using the fault-related frequencies information, the fault diagnosis performance delivered from IESCFFOgram is similar to that of IESFOgram, especially in the analysis of experimental datasets.
- Simulation and experimental analysis indicated that the parameter p1 varying within 1%~10% has a limited influence on the performance of the IESCFFOgram. The parameter p1 ensuring that the IESCFFOgram can more fully identify the informative spectral frequency band to produce diagnostic IES is recommended to set around 5%.

Compliance with ethical standards

Acknowledgments

We thank Eric Bechhoefer, Chief Engineer from NRG systems for sharing the database.

Disclosure of conflict of interest

The authors declare no conflict of interest.

References

[1] Randall RB, Antoni J. Rolling element bearing diagnostics—A tutorial. Me- chanical systems and signal processing. 2011;25(2):485-520.

[2] Tiwari P, Upadhyay SH. Novel self-adaptive vibration signal analysis: Con- cealed component decomposition and its application in bearing fault diagno- sis. Journal of Sound and Vibration. 2021;502:116079.

[3] Lei Y, Li N, Guo L, Li N, Yan T, Lin J. Machinery health prognostics: A systematic review from data acquisition to RUL prediction. Mechanical systems and signal processing. 2018;104:799-834.

[4] Li G, Zhao Q. Minimum entropy deconvolution optimized sinusoidal synthesis and its application to vibration based fault detection. Journal of Sound and Vibration. 2017;390:218-31.

[5] McDonald GL, Zhao Q, Zuo MJ. Maximum correlated Kurtosis deconvolution and application on gear tooth chip fault detection. Mechanical Systems and Signal Processing. 2012;33:237-55.

[6] McDonald GL, Zhao Q. Multipoint optimal minimum entropy deconvolution and convolution fix: application to vibration fault detection. Mechanical Systems and Signal Processing. 2017;82:461-77.

[7] Buzzoni M, Antoni J, d'Elia G. Blind deconvolution based on cyclostationar- ity maximization and its application to fault identification. Journal of Sound and Vibration. 2018;432:569-601.

[8] Cheng Y, Zhou N, Zhang W, Wang Z. Application of an improved mini- mum entropy deconvolution method for railway rolling element bearing fault diagnosis. Journal of sound and vibration. 2018;425:53-69.

[9] Cheng Y, Wang Z, Zhang W, Huang G. Particle swarm optimization algo- rithm to solve the deconvolution problem for rolling element bearing fault diagnosis. Isa Transactions. 2019;90:244-67.

[10] Cheng Y, Chen B, Mei G, Wang Z, Zhang W. A novel blind deconvolution method and its application to fault identification. Journal of Sound and Vibration. 2019;460:114900.

[11] Antoni J, Randall RB. The spectral kurtosis: application to the vibratory surveillance and diagnostics of rotating machines. Mechanical systems and signal processing. 2006;20(2):308-31.

[12] Antoni J. The spectral kurtosis: a useful tool for characterising non-stationary signals. Mechanical systems and signal processing. 2006;20(2):282-307.

[13] Antoni J. Fast computation of the kurtogram for the detection of transient faults. Mechanical Systems and Signal Processing. 2007;21(1):108-24.

[14] Barszcz T, JabL- on´ski A. A novel method for the optimal band selection for vibration signal demodulation and comparison with the Kurtogram. Mechan- ical systems and signal processing. 2011;25(1):431-51.

[15] Moshrefzadeh A, Fasana A. The Autogram: An effective approach for se- lecting the optimal demodulation band in rolling element bearings diagnosis. Mechanical Systems and Signal Processing. 2018;105:294-318.

[16] Peter WT, Wang D. The design of a new sparsogram for fast bearing fault diagnosis: Part 1 of the two related manuscripts that have a joint title as "Two automatic vibration-based fault diagnostic methods using the novel sparsity measurement–Parts 1 and 2". Mechanical Systems and Signal Processing. 2013;40(2):499-519.

[17] Antoni J. The infogram: Entropic evidence of the signature of repetitive transients. Mechanical Systems and Signal Processing. 2016;74:73-94.

[18] Wang D, Peter WT, Tsui KL. An enhanced Kurtogram method for fault diag- nosis of rolling element bearings. Mechanical Systems and Signal Processing. 2013;35(1-2):176-99.

[19] Smith WA, Fan Z, Peng Z, Li H, Randall RB. Optimised Spectral Kurtosis for bearing diagnostics under electromagnetic interference. Mechanical Systems and Signal Processing. 2016;75:371-94.

[20] Wang D. An extension of the infograms to novel Bayesian inference for bear- ing fault feature identification. Mechanical Systems and Signal Processing. 2016;80:19-30.

[21] Antoni J. Cyclostationarity by examples. Mechanical Systems and Signal Processing. 2009;23(4):987-1036.

[22] Wang D, Zhao X, Kou LL, Qin Y, Zhao Y, Tsui KL. A simple and fast guide- line for generating enhanced/squared envelope spectra from spectral coher- ence for bearing fault diagnosis. Mechanical Systems and Signal Processing. 2019;122:754-68.

[23] Wang D, Zhao X, Kou LL, Qin Y, Zhao Y, Tsui KL. A simple and fast guide- line for generating enhanced/squared envelope spectra from spectral coher- ence for bearing fault diagnosis. Mechanical Systems and Signal Processing. 2019;122:754-68.

[24] Schmidt S, Mauricio A, Heyns PS, Gryllias KC. A methodology for identifying information rich frequency bands for diagnostics of mechanical components- of-interest under time-varying operating conditions. Mechanical Systems and Signal Processing. 2020;142:106739.

[25] Mauricio A, Smith WA, Randall RB, Antoni J, Gryllias K. Improved Envelope Spectrum via Feature Optimisation-gram (IESFOgram): A novel tool for rolling element bearing diagnostics under non-stationary operating conditions. Mechanical Systems and Signal Processing. 2020;144:106891.

[26] Mauricio A, Sheng S, Gryllias K. Condition monitoring of wind turbine plan- etary gearboxes under different operating conditions. Journal of Engineering for Gas Turbines and Power. 2020;142(3).

[27] Mauricio A, Qi J, Gryllias K. Vibration-based condition monitoring of wind turbine gearboxes based on cyclostationary analysis. Journal of Engineering for Gas Turbines and Power. 2019;141(3).

[28] Mauricio A, Qi J, Smith WA, Sarazin M, Randall RB, Janssens K, et al. Bearing diagnostics under strong electromagnetic interference based on In- tegrated Spectral Coherence. Mechanical Systems and Signal Processing. 2020;140:106673.

[29] Mauricio A, Gryllias K. Cyclostationary-based multiband envelope spectra extraction for bearing diagnostics: The combined improved envelope spec- trum. Mechanical Systems and Signal Processing. 2021;149:107150.

[30] Chen B, Cheng Y, Zhang W, Gu F, Mei G. Optimal frequency band selec- tion using blind and targeted features for spectral coherence-based bearing diagnostics: A comparative study. ISA transactions. 2021.

[31] Zhang B, Miao Y, Lin J, Li H. Weighted envelope spectrum based on the spectral coherence for bearing diagnosis. ISA transactions. 2022;123:398-412.

[32] Loparo KA. Western Reserve University Bearing Data Center Website; 2020.

[33] Smith W, Borghesani P, Ni Q, Wang K, Peng Z. Data5-3 60Hz-inner. mat. 2019.

[34] Wang B, Lei Y, Li N, Li N. A hybrid prognostics approach for estimating remaining useful life of rolling element bearings. IEEE Transactions on Reli- ability. 2018;69(1):401-12.